ACS Infectious Diseases

Article

pubs.acs.org/journal/aidcbc

Plasmodium IspD (2-C-Methyl-D-erythritol 4-Phosphate Cytidyltransferase), an Essential and Druggable Antimalarial Target

Leah S. Imlay,[†] Christopher M. Armstrong,[‡] Mary Clare Masters,[‡] Ting Li,[§] Kathryn E. Price,[∥] Rachel L. Edwards,[‡] Katherine M. Mann,[†] Lucy X. Li,[†] Christina L. Stallings,[†] Neil G. Berry,[∥] Paul M. O'Neill,[∥] and Audrey R. Odom*[,†,‡]

[†]Department of Molecular Microbiology and [‡]Department of Pediatrics, Washington University School of Medicine, St. Louis, Missouri 63110, United States

[§]College of Medicine, University of Toledo, Toledo, Ohio 43614, United States

[∥]Department of Chemistry, University of Liverpool, Liverpool L69 7ZD, U.K.

Supporting Information

ABSTRACT: As resistance to current therapies spreads, novel antimalarials are urgently needed. In this work, we examine the potential for therapeutic intervention via the targeting of *Plasmodium* IspD (2-C-methyl-D-erythritol 4-phosphate cytidyltransferase), the second dedicated enzyme of the essential methylerythritol phosphate (MEP) pathway for isoprenoid biosynthesis. Enzymes of this pathway represent promising therapeutic targets because the pathway is not present in humans. The Malaria Box compound, MMV008138, inhibits *Plasmodium falciparum* growth, and PfIspD has been proposed as a candidate intracellular target. We find that PfIspD is the sole intracellular target of MMV008138 and characterize the mode of inhibition and target-based resistance, providing chemical validation of this target. Additionally, we find that the *PfISPD* genetic locus is refractory to disruption in malaria parasites, providing independent genetic validation for efforts targeting this enzyme. This work provides compelling support for IspD as a druggable target for the development of additional, much-needed antimalarial agents.

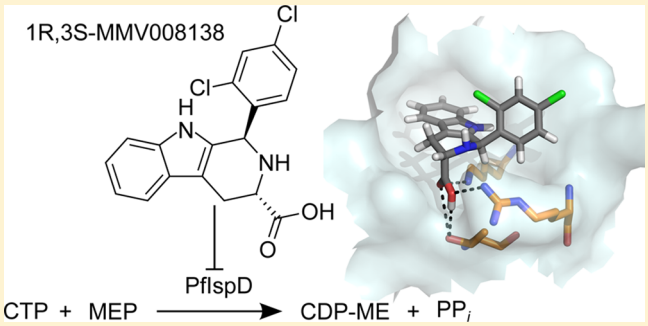

KEYWORDS: *IspD, MEP pathway, MMV008138, plasmodium, malaria, homology model*

Malaria remains a serious global health concern, with over 200 million cases per year and nearly one-half million deaths, primarily in children under the age of 5 and pregnant women.[1] Two species of protozoan parasites contribute the majority of malaria infections: *Plasmodium falciparum*, the most lethal species, and *P. vivax*, a significant cause of morbidity in Asia. The current front-line therapeutics for falciparum malaria are artemisinin-based combination therapies (ACTs). Resistance to ACTs was first described in 2008 and continues to spread rapidly.[2−4] In fact, recent studies indicate that up to 45% of malaria cases are refractory to treatment in some areas of Southeast Asia.[5] There is therefore an urgent need for new antimalarial agents.

Because malaria treatments must be safe for repeated dosing in very young children and during pregnancy, target-based antimalarial drug design depends on the identification of essential parasite processes whose inhibition is unlikely to have human toxicity. One such unique, parasite-specific cellular process is the biosynthesis of isoprenoid precursors. Isoprenoids comprise a large family of biomolecules that are required by all living cells.[6] However, unlike mammalian cells, which generate isoprenoid precursors through the mevalonate pathway, malaria parasites utilize an alternate metabolic route that proceeds through methylerythritol phosphate (MEP).[7] The MEP pathway produces the isoprenoid precursor molecules, isopentenyl pyrophosphate (IPP) and dimethylallyl pyrophosphate (DMAPP), through seven enzymatic steps. The first dedicated step of this pathway is the synthesis of the key metabolite, MEP, by enzyme DXR (E.C. 1.1.1.267, MEP synthase). In the subsequent reaction, IspD (E.C. 2.7.7.60, MEP cytidyltransferase) catalyzes the cytidylation of MEP to cytidine diphosphate methylerythritol (CDP-ME). Because the inhibition of DXR dramatically reduces IspD function in cells, IspD may represent a point of particular metabolic control of MEP pathway flux.[8]

The clinical symptoms of malaria are a result of asexual reproduction of the parasite within human erythrocytes. Blood-stage parasites may also develop into male and female sexual stages (gametocytes), whose uptake by and subsequent development within the *Anopheles* mosquito are necessary for malaria transmission. Evidence suggests that the MEP pathway

Received: December 17, 2014
Published: March 2, 2015

DOI: 10.1021/id500047s
ACS Infect. Dis. 2015, 1, 157−167

is required for the development of both asexual intraerythrocytic parasites and gametocytes. Metabolic studies have repeatedly demonstrated that the MEP pathway is active within asexual parasites,[8−10] and a recent study has established that this pathway is active within gametocytes as well.[11] In addition, the locus encoding DXR, the first dedicated enzyme of the MEP pathway, is resistant to disruption in *P. falciparum*, providing further genetic validation that flux through the MEP pathway is required for parasite development.[12]

Phosphonic acid antibiotic fosmidomycin is a substrate mimic and inhibitor of DXR.[13] The inhibition of downstream enzyme IspD is also metabolically apparent in fosmidomycin-treated cells, although IspD homologues are not directly inhibited by fosmidomycin in vitro.[8] Fosmidomycin is an effective antimalarial agent and is currently in phase II clinical trials in combination therapy with piperaquine.[14] The safety profile of fosmidomycin is impressive, with a mouse LD_{50} of >11 000 mg/kg and no adverse events noted in phase I or II clinical trials.[15−19] Although the pharmacokinetics of fosmidomycin are suboptimal,[20−23] this compound demonstrates the promise of future MEP pathway inhibitors to deliver a safe new antimalarial therapeutic.

The antimalarial activity of MMV008138 [(2,4-dichlorophenyl)-2,3,4,9-tetrahydro-1*H*-pyrido[3,4-*b*]indol-2-ium-3-carboxylate)] was first recognized through phenotypic screening of the large screening library of GlaxoSmithKline.[24] Several antimalarial compounds, including MMV008138 from this and other screening efforts, have been generously made available free of charge to the scientific community by the Medicines for Malaria Venture (MMV) as part of the Malaria Box.[25] MMV008138 has emerged as a Malaria Box compound of particular interest because its antiparasitic activity is reduced when parasites are supplemented with an exogenous supply of the isoprenoid building block, IPP.[26] This finding strongly suggested that the antiparasitic activity of MMV008138 was mediated through inhibition of the MEP pathway. Recently, Wu et al. determined that the 1R,3S diastereomer of MMV008138 is most active and generated three 1*R*,3*S*-MMV008138-resistant *P. falciparum* strains.[27] Each strain contained a nonsynonymous mutation in PF3D7_0106900, which encodes IspD. Furthermore, 1*R*,3*S*-MMV008138 directly inhibited purified recombinant *P. falciparum* IspD (PfIspD). Thus, PfIspD has been proposed as a candidate intracellular target of 1*R*,3*S*-MMV008138[27] (Scheme 1).

In this article, we examine the potential for therapeutic intervention against malaria infection via inhibition of PfIspD. We establish that PfIspD represents the enzymatic target of 1*R*,3*S*-MMV008138 and demonstrate that 1*R*,3*S*-MMV008138 inhibits PfIspD competitively with its CTP substrate. The inhibition of bacterial IspD orthologs was not observed, but *P. vivax* IspD is inhibited, suggesting that further modifications to this scaffold may widen its therapeutic scope against multiple malaria species. To support these and similar studies, we have also genetically validated *PfISPD* as an essential gene. These studies provide strong biological support for ongoing antimalarial development targeting PfIspD. The MEP pathway in general and IspD in particular represent a key opportunity to develop well-tolerated therapeutics for the treatment of malaria.

RESULTS AND DISCUSSION

1*R*,3*S*-MMV008138 Inhibits Isoprenoid Biosynthesis in *Plasmodium falciparum*. 1*R*,3*S*-MMV008138 inhibits the growth of cultured *P. falciparum* and also reduces the activity of

Scheme 1. IspD Reaction and Proposed Inhibition by 1*R*,3*S*-MMV008138

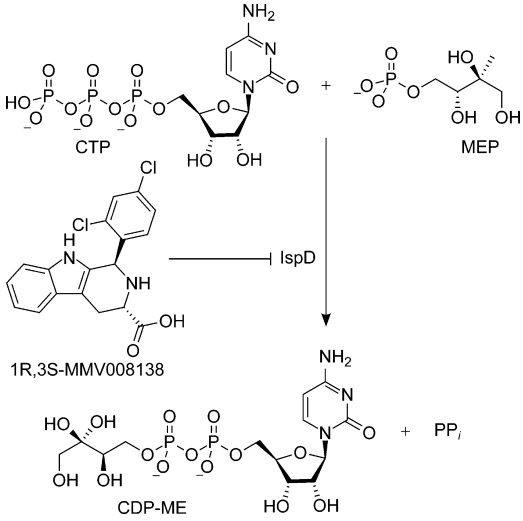

purified recombinant PfIspD protein, whereas the 1S,3R diastereomer is inactive.[27] Inhibition of IspD in vivo by 1*R*,3*S*-MMV008138 is therefore hypothesized to result in decreased cellular levels of metabolites enzymatically downstream from IspD. To establish the antiparasitic mechanism of action of 1*R*,3*S*-MMV008138, we performed targeted metabolic profiling of MEP pathway metabolites in *P. falciparum* cells treated for 12 h with 1.5 μM MMV008138 (5 times the EC_{50}) using quantitative liquid chromatography−mass spectrometry (LC−MS/MS, Figure 1). In addition, we quantified MEP

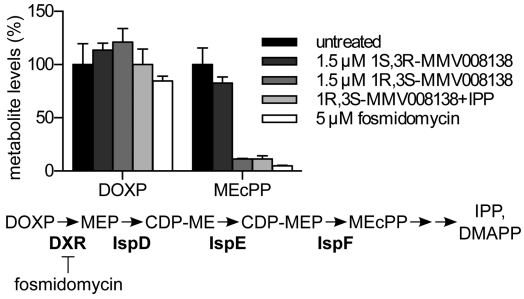

Figure 1. 1*R*,3*S*-MMV008138 inhibits isoprenoid biosynthesis in malaria parasites. MEP metabolites [deoxyxylulose phosphate (DOXP, upstream from IspD) and methylerythritol cyclic diphosphate (MEcPP, downstream from IspD)] were quantified by LC-MS/MS from *P. falciparum* parasites, following treatment with the indicated agents: fosmidomycin, positive control (known DXR inhibitor); 1*S*,3*R*-MMV008138, inactive diastereomer; and 1*R*,3*S*-MMV008138, active diastereomer whose antiparasitic effects are relieved by cotreatment with downstream isoprenoid IPP. Data are normalized to untreated controls and represent three independent biological replicates. Below is shown a schematic of the selected MEP pathway enzymes and metabolites, including DOXP and MEcPP.

metabolites in untreated, IPP-rescued, and fosmidomycin-treated parasites. None of these conditions caused significant changes in the levels of DOXP, which is metabolically upstream from both DXR and IspD. As previously described,[8] fosmidomycin treatment of *P. falciparum* caused a 95 ± 2% decrease in the cellular levels of the most distal MEP metabolite detected, methylerythritol cyclic diphosphate (MEcPP) (unpaired *t* test, $p < 0.005$). Similarly, we found that 1*R*,3*S*-

DOI: 10.1021/id500047s
ACS Infect. Dis. 2015, 1, 157−167

MMV008138 treatment of *P. falciparum* also dramatically reduced levels of MEcPP to 12 ± 4% of control levels (unpaired *t* test, $p < 0.005$), consistent with the inhibition of the cellular MEP pathway metabolism upstream from MEcPP. This effect on cellular MEcPP levels was not observed with the inactive 1S,3R diastereomer of MMV008138. Importantly, 1*R*,3*S*-MMV008138-treated parasites supplemented with 200 μM IPP are viable, but 1*R*,3*S*-MMV008138 treatment of such IPP-rescued cells still results in a significant reduction in MEcPP levels (unpaired *t* test, $p < 0.005$). This result indicates that decreased levels of MEcPP in 1*R*,3*S*-MMV008138-treated parasites are not a result of cell death but are a specific result of inhibitor treatment. As an additional control, *P. falciparum* parasites were treated with one of the unrelated antimalarial compounds chloroquine (28 nM) or artemisinin (20 nM). No effect on MEP pathway metabolite levels was observed (Figure S1), establishing that the metabolic effects of 1*R*,3*S*-MMV008138 are specific to MEP pathway inhibition. Because the antimalarial effects of this compound are rescued by media supplementation with MEP pathway product IPP,[26] together these studies strongly support that 1*R*,3*S*-MMV008138 inhibits malaria parasite growth as a consequence of MEP pathway inhibition.

MMV008138-Resistant Alleles of IspD Confer Resistance in Vitro. Single nucleotide polymorphisms in PF3D7_0106900 (encoding PfIspD) have previously been identified from *P. falciparum* parasite lines selected for MMV008138 resistance in culture.[27] For this reason, IspD was proposed to be a candidate cellular target of MMV008138. Although metabolic profiling confirms that 1*R*,3*S*-MMV008138 inhibits cellular isoprenoid biosynthesis, it cannot distinguish the mode or target of inhibition. For example, changes in IspD function in the 1*R*,3*S*-MMV008138-resistant variants might confer resistance directly by altering interactions with the inhibitor or alternatively may confer resistance through indirect cellular mechanisms.

Two distinct mutations were identified in 1*R*,3*S*-MMV008138-resistant strains: L244I and E688Q.[27] Because these residues are not highly conserved and neither of these mutations is localized to the active site, the mechanism by which these changes could directly alter the sensitivity to 1*R*,3*S*-MMV008138 was unclear. To establish whether PfIspD represents the direct cellular target of 1*R*,3*S*-MMV008138, we cloned and purified recombinant PfIspD proteins with each of the 1*R*,3*S*-MMV008138-resistant alleles. To evaluate the function of the mutant enzymes, kinetic parameters (k_{cat}, K_m) were characterized for each variant (Table S1). The in vitro sensitivity of each variant enzyme to 1*R*,3*S*-MMV008138 was evaluated and compared to that of the wild-type protein (Figure 2). As previously described,[27] we found that 1*R*,3*S*-MMV008138 potently inhibited purified recombinant wild-type PfIspD, with a half-maximal inhibitory concentration (IC_{50}) of 47 nM (95% CI 37−60 nM). In contrast, both PfIspD-L244I and PfIspD-E688Q proteins demonstrated resistance to 1*R*,3*S*-MMV008138 in vitro, as quantified by significantly increased IC_{50} values [E688Q, 100 nM (95% CI 82−130 nM); L244I, 320 nM (95% CI 200−530 nM); $p < 0.0001$ for both, unpaired *t* test]. Notably, the resistance observed in purified mutant proteins was found to parallel that of the MMV008138-resistant *P. falciparum* lines in which these mutations were identified such that the E688Q allele is associated with 3.5-fold 1*R*,3*S*-MMV008138 resistance in vivo, whereas parasites with the L244I allele are >10-fold more resistant than the parental

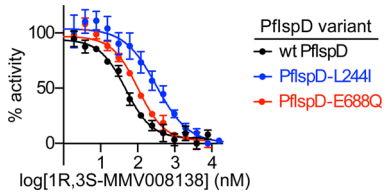

Figure 2. MMV008138-resistant variants of PfIspD confer resistance in vitro. Dose-dependent inhibition of purified recombinant wild-type (wt) and resistant variants of PfIspD by 1*R*,3*S*-MMV008138. Each data point represents at least three independent experiments and is presented as the mean ± SEM. Data are normalized to activity observed in the absence of 1*R*,3*S*-MMV008138.

strain.[27] Because protein polymorphisms that confer phenotypic resistance also confer resistance in vitro, these data strongly indicate that PfIspD directly interacts with 1*R*,3*S*-MMV008138 as the primary intracellular target responsible for antiparasitic activity. PfIspD therefore represents a druggable target for *P. falciparum*, and 1*R*,3*S*-MMV008138 shows promise as a potential scaffold for target-based antimalarial drug development.

1*R*,3*S*-MMV008138 Is Competitive with CTP but Not MEP. IspD catalyzes the transfer of a cytidyl group from CTP to methylerythritol phosphate and therefore utilizes two substrates, MEP and CTP. To understand the molecular mechanism by which 1*R*,3*S*-MMV008138 inhibits PfIspD activity, we performed a kinetic characterization of the enzyme under a range of inhibitor concentrations (Figure 3, Table S1).

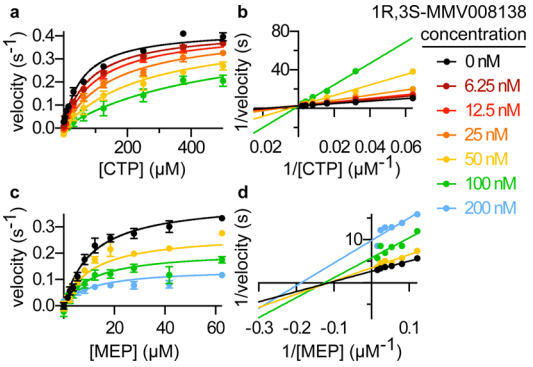

Figure 3. Inhibition of PfIspD by 1*R*,3*S*-MMV008138 is competitive with CTP but not MEP. (a) Kinetic parameters with respect to the CTP substrate. Each data point represents mean ± SEM from at least three independent experiments. (b) Lineweaver−Burk double-reciprocal plots of wild-type PfIspD activity over a range of CTP substrate concentrations, for illustrative purposes only. (c) Kinetic parameters with respect to the MEP substrate. Each data point represents the mean ± SEM from at least three independent experiments. (d) Lineweaver−Burk double-reciprocal plots of wild-type PfIspD activity over a range of MEP substrate concentrations, for illustrative purposes only.

Although the *Plasmodium* IspD homologues have substantial sequence divergence from their bacterial and plant orthologs, the Michaelis constant (K_m) of purified recombinant PfIspD is similar to those previously described for other IspD enzymes (Table S1).[28−30] We find that 1*R*,3*S*-MMV008138 is noncompetitive with respect to the MEP substrate. Analysis using the corrected Akaike's Informative Criterion (AICc) supports a noncompetitive rather than competitive model of inhibition (>99.99% probability). In contrast, the same comparison

DOI: 10.1021/id500047s
ACS Infect. Dis. 2015, 1, 157−167

strongly supports a model of competitive inhibition of PfIspD with respect to CTP (>99.99% probability), with a K_i[CTP] for 1*R*,3*S*-MMV008138 of 14 ± 1.3 nM.

Similar kinetic analyses were performed for the two 1*R*,3*S*-MMV008138-resistant PfIspD variant proteins (Figure S3, Table S1). Although the PfIspD-E688Q mutation did not significantly alter the K_i[CTP] for 1*R*,3*S*-MMV008138 (17 ± 1.7 nM, S.E.; $p = 0.17$, unpaired t test), this variant does have a slightly higher k_{cat}[CTP] than for the wild-type enzyme (0.50 ± 0.0078 s^{-1}; $p < 0.0001$, unpaired t test) and a substantially lower K_m[CTP] (27 ± 2.1 nM, S.E.; $p < 0.0001$, unpaired t test). The decreased K_m[CTP] suggests that 1*R*,3*S*-MMV008138 may compete poorly against CTP to bind PfIspD-E688Q, compared to the wild-type enzyme.

The second resistant variant, PfIspD-L244I, also exhibits a significantly decreased K_m[CTP] (16 ± 1.9 nM, $p < 0.0001$, unpaired t test). Additionally, the K_i[CTP] for MMV008138 is dramatically increased (130 ± 26 nM, $p < 0.0001$, unpaired t test), likely reflecting a much lower affinity for the inhibitor. Of note, the k_{cat} (0.16 ± 0.0045 s^{-1}, S.E.) is decreased by approximately 4-fold compared to that of wild-type PfIspD ($p < 0.0001$, unpaired t test).

1*R*,3*S*-MMV008138 Is Active against *P. vivax* but Not Bacterial IspD Homologues. The MEP pathway is evolutionarily ancient, and its enzymes are highly conserved among eubacteria and plastid-containing eukaryotes. Newly identified MEP pathway inhibitors are therefore of considerable interest as potential antibacterial or antimycobacterial agents, in addition to their promise as treatments for *P. falciparum* and *P. vivax* infections.[31] To evaluate the potential antimicrobial spectrum and species selectivity of 1*R*,3*S*-MMV008138, we examined its activity against diverse IspD orthologs (Figure 4).

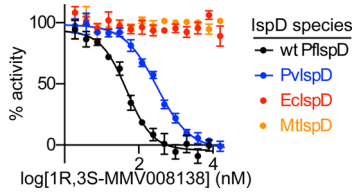

Figure 4. Species selectivity of 1*R*,3*S*-MMV008138 against IspD orthologs. Dose-dependent inhibition of purified recombinant IspD orthologs from *P. falciparum* (Pf), *P. vivax* (Pv), *E. coli* (Ec), and *M. tuberculosis* (Mt). Each data point represents at least three independent experiments (mean ± S.E.M). Data are normalized to the activity observed in the absence of 1*R*,3*S*-MMV008138.

As previously reported, 1*R*,3*S*-MMV008138 does not inhibit *Escherichia coli* IspD at concentrations <30 μM. In addition, we find that *Mycobacterium tuberculosis* IspD (MtIspD) is also insensitive to 1*R*,3*S*-MMV008138. In contrast to previously reported results, we find that *P. vivax* IspD (PvIspD) is potently inhibited by 1*R*,3*S*-MMV008138 (IC_{50} 310 nM, 95% CI 240–400 nM), although PfIspD remains the most sensitive IspD ortholog evaluated. It is likely that the low (50 μM) CTP concentration used in our assays supported more obvious PvIspD inhibition than was previously observed.[27] Kinetic studies indicate that, as seen for PfIspD, the inhibition of PvIspD occurs via competition with the CTP substrate (Figure S3, Table S1).

Modeling of 1*R*,3*S*-MMV008138 in the *P. falciparum* CTP Binding Site. In addition to in vitro and cellular analysis of 1*R*,3*S*-MMV008138 inhibition, molecular modeling studies were undertaken to provide insight as to how the compound may bind to its IspD enzymatic target. A homology model of PfIspD was created using PHYRE and was assessed to have 98.92% confidence.[32] After validation using the WHATIF web interface, the model was used to dock 1*R*,3*S*-MMV008138 within the CTP binding site using GOLD in order to assess the strength of interactions and to visualize the noncovalent contacts between our inhibitor and the binding site (Figure 5).[33,34]

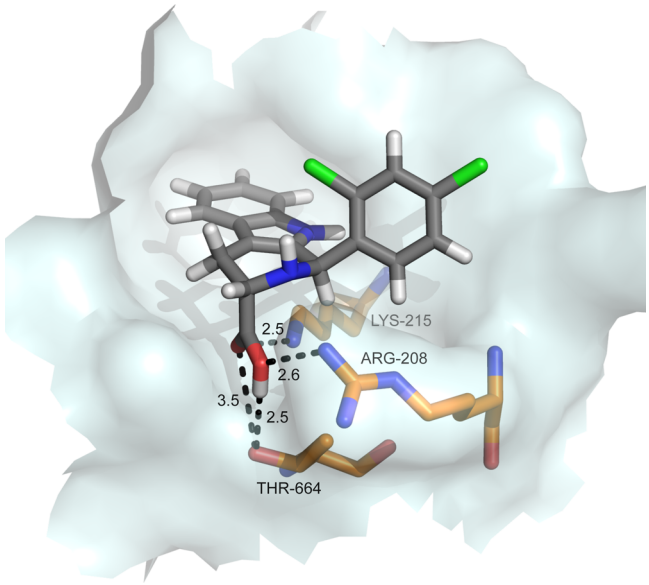

Figure 5. Docking pose of 1*R*,3*S*-MMV008138 in the homology model of PfIspD. The active site is rendered as a white surface, and residues forming hydrogen bonds with 1*R*,3*S*-MMV008138 are depicted as sticks (carbon, orange; oxygen, red; nitrogen, blue). 1*R*,3*S*-MMV008138 rendered as sticks (carbon, gray; oxygen, red; nitrogen, blue; hydrogen, white). Hydrogen bonds are shown as dotted black lines, with distance given in angstroms. Image created using PyMOL (The PyMOL Molecular Graphics System, version 1.5.0.4, Schrödinger, LLC).

The inhibitor, 1*R*,3*S*-MMV008138, was predicted to bind within the enzyme active site, with an average GoldScore of 49.6 ± 3. 1*R*,3*S*-MMV008138 has an excellent spatial fit in the active site of the PfIspD structure and mimics the binding mode of the cytidine phosphate moiety in the *E. coli* crystal structure (PDB 1I52).[35] 1*R*,3*S*-MMV008138 is predicted to form an array of four hydrogen bonds between its carboxylic acid and T664, R208, and K215; these mirror those formed by the phosphate group in 1I52 and are supportive of the competitive nature of this compound with CTP, as observed enzymologically. The stereochemical requirement for the 1R,3S disastereomer can be rationalized through the spatial demands of the binding site, as shown by the enzyme surface rendered in Figure 5. CTP has a GoldScore of 72.0 ± 4. The higher GoldScore of CTP is largely ascribed to the greater negative charge on the triphosphate group compared to that of the 1*R*,3*S*-MMV008138 compound. Predictions based on this docking model await structural verification. An examination of residues in the binding site will enable the design of future generations of compounds with even greater potency.

***PfISPD* (PF3D7_0106900) Is Resistant to Genetic Disruption.** Chemical validation of drug targets can be misleading, as was previously described for the candidate

DOI: 10.1021/id500047s
ACS Infect. Dis. 2015, 1, 157–167

antimalarial target of triclosan, FabI, which was ultimately found to be dispensable in blood-stage malaria parasites.[36,37] Although our studies strongly suggest that 1*R*,3*S*-MMV008138 is a specific inhibitor of PfIspD, we sought to validate this antimalarial target independently. Because the malaria parasite is haploid during the intraerythrocytic cycle, essential loci cannot be disrupted. For this reason, we pursued a single-crossover strategy to determine whether *PfISPD* can be disrupted in cultured *P. falciparum* parasites, as was previously used to validate the antimalarial target of fosmidomycin, *PfDXR*[12] (Figure S4). Single-crossover pCAM-BSD-derived vectors were designed to integrate by homologous recombination at the PF3D7_0106900 locus, which encodes PfIspD. Integration of the disruptant vector (pCAM-BSD-PfIspD^{KO}) was engineered to interrupt the expression of functional PfIspD. Integration of the control vector (pCAM-BSD-PfIspD^{control}) was designed to preserve gene function by recapitulating the full-length gene upon integration.

The growth of blasticidin-resistant parasites was apparent approximately 1 month following transfection with either vector. A single line of parasites transfected with pCAM-BSD-PfIspD^{control} was obtained (C1); integration of this control plasmid was confirmed by PCR and Southern blot analysis within 2 months post-transfection, confirming that the *PfISPD* locus is amenable to genetic manipulation. In contrast, two independent lines of parasites transfected with pCAM-BSD-PfIspD^{KO} were obtained (KO1 and KO2). Both lines were continuously cultured for up to 6 months and were cycled off and on blasticidin-selective pressure, without evidence of integration by PCR or Southern blot (Figure 6, Figure S4). These results indicate that the disruption of *PfISPD* gene function does not support parasite growth. Together, our chemical and genetic validation experiments provide separate lines of evidence that intraerythrocytic survival of the malaria parasite depends on *PfISPD* function, fully validating IspD as an essential, parasite-specific target for antimalarial drug development.

Fosmidomycin and 1*R*,3*S*-MMV008138 Have Additive Antiparasitic Activity. Antimalarial combination therapy is necessary to prevent the development and spread of antimalarial drug resistance. Potential drug combinations may be antagonistic, for example, when one compound reduces the import of another. We therefore explored the possibility for antagonism or synergy between 1*R*,3*S*-MMV008138 and the canonical MEP inhibitor, fosmidomycin, using a modified fixed-ratio isobole method.[38] The isobole generated is approximately linear (Figure 7), suggesting that the antimalarial actions of fosmidomycin and 1*R*,3*S*-MMV008138 are additive. These data were also quantified through the calculation of sum fractional inhibitory concentrations (sum FICs),[39] in which sum FIC values <0.5 reflect synergy and sum FIC values >2 indicate antagonism. We find that the sum FIC value of 1*R*,3*S*-MMV008138 and fosmidomycin was 0.88 ± 0.062 (mean and standard deviation), also supporting additivity (no substantial interaction) between fosmidomycin and 1*R*,3*S*-MMV008138.

Fosmidomycin Resistance Does Not Also Confer Resistance to MMV008138. *P. falciparum* strains that lack sugar phosphatase PfHAD1 have increased levels of MEP metabolites, including DOXP and MEP, and are resistant to DXR inhibitor fosmidomycin.[40] Because IspD inhibitor 1*R*,3*S*-MMV008138 is competitive with CTP but not MEP, we predicted that HAD1 loss of function would not confer resistance to 1*R*,3*S*-MMV008138. We therefore evaluated the

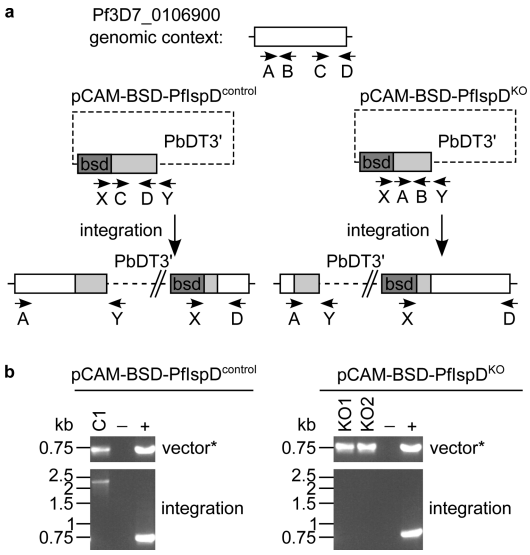

Figure 6. Genetic analysis of pCAM-BSD-IspD transfectants. (a) Strategy for single-crossover disruption of the *PfISPD* locus, PF3D7_0106900. Transfection plasmids contain inserts homologous to the coding sequences for either the C-terminus (positions 1543−2205, pCAM-BSD-PfIspD^{control}, left) or an N-terminal section (positions 17−645, pCAM-BSD-PfIspD^{KO}, right) of PfIspD. Integration of the control vector is expected to recapitulate normal gene function, whereas integration of the knockout vector would disrupt functional PfIspD expression. Primers used in diagnostic PCRs are shown as arrows. *Acc*I restriction sites are depicted with the letter *a*, *Pst*I restriction sites are depicted with the letter *p*, and *Sma*I restriction sites are depicted with the letter *s*. (b) Diagnostic PCR reactions to assess genomic integration of control (pCAM-BSD-PfIspD^{control}) and disruption (pCAM-BSD-PfIspD^{KO}) vectors. Genomic DNA isolated from parasites transfected with either vector was subjected to amplification with the indicated primers. For pCAM-BSD-PfIspD^{control}-transfected parasites (C1), primers X + Y would detect vector DNA (negative control, untransfected 3D7; positive control, pCAM-BSD-PfIspD^{control} plasmid), and primers A + Y are integration-specific (negative control, untransfected 3D7; positive control, pCAM-BSD-PfIspD^{KO} plasmid). For pCAM-BSD-PfIspD^{KO}-transfected parasites (KO1 and KO2), primers X + Y would detect vector DNA (negative control, untransfected 3D7; positive control, pCAM-BSD-PfIspD^{KO} plasmid), whereas primers A + Y are integration-specific (negative control, untransfected 3D7; positive control, pCAM-BSD-PfIspD^{control} plasmid). *, vector bands may indicate either episomal plasmids or integrated concatamers.

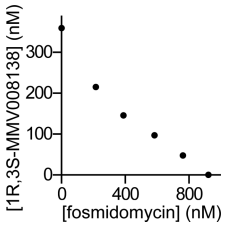

Figure 7. Antiparasitic effects of 1*R*,3*S*-MMV008138 and fosmidomycin are additive, not synergistic. Parasite growth was assayed after cotreatment with a variety of 1*R*,3*S*-MMV008138 and fosmidomycin concentrations. Pairs of concentrations (e.g., ([fosmidomycin], [1*R*,3*S*-MMV008138]) at which 50% growth inhibition was observed (EC_{50}) are plotted. A linear isobole indicates additive antiparasitic activity. Data points above represent averages from at least three independent experiments.

DOI: 10.1021/id500047s
ACS Infect. Dis. 2015, 1, 157−167

growth sensitivity of HAD1 loss-of-function strain AM1 compared to complemented strain AM1 expressing HAD1-GFP (AM1 Hsp110: PfHAD1-GFP), which restores both fosmidomycin sensitivity and MEP metabolite levels (Figure 8).

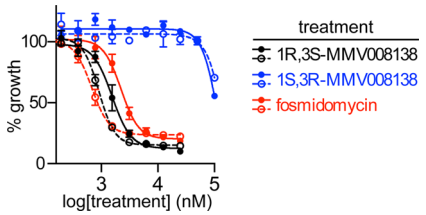

Figure 8. Fosmidomycin resistance does not confer MMV008138 resistance. Dose-dependent growth inhibition by 1*R*,3*S*-MMV008138 (active diastereomer), 1*S*,3*R*-MMV008138 (inactive diastereomer), and fosmidomycin was determined for the fosmidomycin-resistant PfHAD1 loss-of-function parasite strain (AM1; solid circles and lines) and the fosmidomycin-sensitive complemented strain (AM1 Hsp110: PfHAD1-GFP; open circles and dashed lines). Data (mean ± S.E.M.) are representative of at least three independent biological replicates and are normalized to growth in the absence of treatment.

We find that HAD1 loss of function did not confer significant resistance to 1*R*,3*S*-MMV008138 [AM1 EC_{50}: 1.3 μM (95% CI 0.67−2.5 μM); AM1 Hsp110: PfHAD1-GFP EC_{50}: 0.87 μM (95% CI 0.53−1.4 μM); p = 0.11, unpaired t test]. These results are consistent with competition with the CTP substrate, rather than MEP, as a mode for 1*R*,3*S*-MMV008138 inhibition. In addition, these findings indicate that the primary mechanisms of resistance for 1*R*,3*S*-MMV008138 (target mutation) and fosmidomycin (metabolic regulation) do not overlap. Thus, our studies provide reassurance that resistance to a single MEP pathway inhibitor may not always confer cross-resistance to others, a finding that may influence future decision making about potential antimalarial partner agents for novel MEP pathway inhibitors as they are developed.

Large-scale phenotypic screening for new antimalarials has led to the identification of over 14 000 new compounds with selective activity against cultured *P. falciparum* malaria parasites.[24,41] For the majority of these chemical entities, the cellular target and mechanism of action are yet unknown. As underlined here, these compounds not only represent chemical scaffolds that may be suitable for antimalarial drug development but also serve as probe molecules, the study of which promises to illuminate essential parasite functions that are, by definition, amenable to small-molecule inhibition.

Our work has established MEP pathway enzyme PfIspD as the target of the active 1R,3S diastereomer of one such hit compound, MMV008138, and has established the mode of inhibition. 1*R*,3*S*-MMV008138 represents a promising chemotype to explore for potential antimalarial drug development. Because MMV008138 has been included in the Malaria Box, multiple biological screens have been performed (summarized: https://www.ebi.ac.uk/chembl/malaria/compound/inspect/CHEMBL527593). MMV008138 is active against both chloroquine-sensitive and -resistant lines of *P. falciparum*, and its growth inhibitory activity appears to be limited to intraerythrocytic *Plasmodium* spp. Specifically, MMV008138 does not appreciably inhibit the growth of either multiple human cells lines (HepG2, Huh7, and fibroblasts) or unrelated parasitic species (*Leishmania infantum* and *Schistosoma mansoni*), none of which possess the MEP pathway.[24,42−44]

Unfortunately, MMV008138 does not exhibit activity against liver-stage *P. yoelii* nor does it have activity against sexual-stage gametocytes of *P. falciparum*.[26,45−49] This lack of activity against extraerythrocytic forms of the parasite does not necessarily indicate that IspD function is not required during those stages. Recent studies have demonstrated that the MEP pathway is metabolically active during gametocytogenesis, and fosmidomycin, the canonical MEP pathway inhibitor, inhibits liver-stage development of *P. berghei*.[11,50] The most parsimonious explanation of the lack of activity during gametocytogenesis is that 1*R*,3*S*-MMV008138, like many compounds, has decreased cell permeability during these life-cycle stages, particularly because IPP production appears to be required for efficient gametocytogenesis and survival.[11] Development projects aiming to target other stages of the parasite life cycle may therefore necessitate modification of 1*R*,3*S*-MMV008138 to improve cellular permeability while preserving interactions with IspD.

Previous studies have demonstrated that IspD orthologs in other organisms are amenable to small-molecule inhibition.[51,52] Notably, prior efforts to identify IspD inhibitors have yet to identify an inhibitor class with broad antimicrobial action. 1*R*,3*S*-MMV008138 represents the most potent IspD inhibitor described to date and has similarly narrow species specificity. In contrast to previously described allosteric inhibitors, 1*R*,3*S*-MMV008138 appears to target the CTP binding site of PfIspD. Nucleotide binding sites have historically had great success as targets for clinical agents for such diverse therapeutic areas as HIV, hepatitis B, and cancer.[53−55] In fact, there has been a recent explosion of FDA-approved small-molecule kinase inhibitors, most of which specifically target ATP binding sites of individual human kinases,[56,57] highlighting the potential for selectivity in targeting nucleotide binding regions. The in vitro and cellular specificity we find with 1*R*,3*S*-MMV008138 suggests that the CTP binding site of PfIspD may likewise be safely targeted, with this scaffold representing an excellent starting point for structure-based drug design efforts.

METHODS

MEP Metabolite Profiling. Asynchronous cultures of *P. falciparum* strain 3D7 were treated for 12 h with 1.5 μM 1*R*,3*S*-MMV008138, 1.5 μM 1*S*,3*R*-MMV008138, 1.5 μM 1*R*,3*S*-MMV008138, and 200 μM IPP or 5 μM fosmidomycin (5 times the EC_{50} value for each compound) and compared to untreated controls. Prior to artemisinin or chloroquine treatment, parasites were grown to >8% parasitemia and synchronized with 5% sorbitol to >75% ring-stage parasites. After 48 h (one cell cycle), parasites were treated for 10 h with 20 nM artemisinin or 28 nM chloroquine or were left untreated. Following treatment, parasite-infected erythrocytes were lysed with 0.1% saponin, washed in phosphate-buffered saline, and stored at −80 °C until extraction and quantitative LC−MS/MS measurement of DOXP and MEcPP, as previously described.[8] Values reflect the mean and standard deviations of at least three independent experiments.

Cloning of PfIspD and Orthologs. *P. falciparum.* A synthetic gene encoding *PfISPD* (PF3D7_0106900), codon-optimized for *E. coli* expression, was generated by GenScript (Piscataway, NJ) in which the N-terminal apicoplast localization sequence was truncated (gene sequence and protein sequence provided in Supporting Information) and cloned into pUC-57. Codon-optimized *PfISPD* was subsequently PCR amplified using primers (PfIspD Fwd primer: 5′-CTCACC-

DOI: 10.1021/id500047s
ACS Infect. Dis. 2015, 1, 157−167

ACCACCACCACCATATGATGCACATCTACGATAATAA-TAA-3′; PfIspD Rev: 5′-ATCCTATCTTACTCACTTATT-TTGAGGAGTAGTAGAAT-3′), cloned into pBG1869 by ligation-independent cloning as previously described[58] and verified by Sanger sequencing. This plasmid introduces an N-terminal 6-His tag for nickel affinity purification.

To generate PfIspD variants containing either the E688Q or the L244I mutation, N- and C-terminal fragments of the optimized *PfISPD* gene were amplified using the following primers: L244I N-terminal fragment, PfIspD Fwd primer with 5′-CTGAAATGTTTTTTATCGCAAACTATAGTCAGG-GATTTGATCAGGTTAC-3′; L244I C-terminal fragment, 5′-GTAACCTGATCAAATCCCTGACTATAGTTTGCGAT-AAAAAACATTTCAG-3′ with PfIspD Rev primer; E688Q N-terminal fragment, PfIspD Fwd primer with 5′-CGTCTTTGA-AGATACTTTCTTGGATATCGATGAATTTGTAGTTG-3′; E688Q C-terminal fragment, 5′-CAACTACAAATTCATCGA-TATCCAAGAAAGTATCTTCAAAGACG-3′ with PfIspD Rev primer. Amplicons containing the entire *PfISPD* gene were generated using PfIspD Fwd and Rev primers, with N- and C-terminal fragments as templates. Following amplification, *PfISPD* variants were cloned into pBG1861 as above and verified by Sanger sequencing.

P. vivax. As for wild-type PfIspD, a synthetic gene encoding codon-optimized *PvISPD* (*P. vivax* Sal-1; PVX_081425) was synthesized by GenArt (Life Technolgies), with a truncated N-terminal apicoplast localization sequence (gene and protein sequences provided in Supporting Information). This construct was cloned into pUC-57. The codon-optimized *PvISPD* gene was amplified using 5′-CTCACCACCACCACCACCATC-CGCGTCTGTTTGAAACCACC-3′ and 5′-ATCCTATCT-TACTCACTTATTCATAATAGAAATGACGATACA-3′. Following amplification, *PvISPD* was cloned into pBG1861 and verified by Sanger sequencing.

Mycobacterium tuberculosis. The *ispD* gene (*Rv3582c*) was amplified from the *Mycobacterium tuberculosis* Erdman strain with primers 5′-GAAGCTTTCACCCGCGCACTATAGC-TTG-3′ and 5′-GGGATCCGTGGTCAGGGAAGCGGGC-3′ and cloned into the *Bam*HI and *Hin*dIII sites of the pETSUMO vector (Invitrogen, Life Technologies) to generate the pETSUMO-IspD expression plasmid, which was verified by Sanger sequencing.

Purification of IspD Proteins. Plasmodium and *E. coli*. Plasmids derived from pBG1861, containing wild-type or mutant alleles of *Plasmodium* IspD, were used to transform Artic Express (DE3) RIL *E. coli* cells (Stratagene). Cells were grown in LB broth with 100 μg/mL ampillicin at 37 °C and 200 rpm. At mid-logarithmic growth, cultures were cooled to 8 °C, and protein expression was induced with 1 mM IPTG for 15 h. *E. coli* IspD was expressed using the pBG-IspD plasmid[8] and transformed into BL21 (DE3) Star *E. coli* cells (Invitrogen, Life Technologies). Cells were grown in LB broth with 100 μg/mL ampillicin at 37 °C and 200 rpm. At mid-logarithmic growth, protein expression was induced with 1 mM IPTG for 2 h.

After induction, cell pellets from the expression of PfIspD were lysed by sonication in lysis buffer (25 mM Tris pH 7.5, 250 mM NaCl, 1 mM $MgCl_2$, 1 mM dithiothreitol (DTT), 20 mM imidazole, 10% glycerol, 0.1% Triton X-100, 200 μM PMSF, 1 mg/mL lysozyme, 0.3 U/mL benzonase nuclease (Novagen), and Roche Complete EDTA-free protease inhibitor). 6-His-tagged IspD proteins were purified from soluble lysate over Ni-NTA resin (Goldbio). Beads were washed with 250 mM NaCl, 25 mM Tris pH 7.5, 1 mM $MgCl_2$, 20 mM imidazole, and 10% glycerol, and protein was eluted with 250 mM NaCl, 25 mM Tris pH 7.5, 1 mM $MgCl_2$, 300 mM imidazole, and 10% glycerol. Affinity purification of PvIspD proceeded similarly to PfIspD purifications, except that 0.1% Triton X-100 was not present in the lysis buffer and 10% glycerol was absent from all buffers. Affinity purification of EcIspD was also performed using a similar protocol, but lysis buffer contained 10 mM Tris pH 7.5, 200 mM NaCl, 1 mM $MgCl_2$, 1 mM dithiothreitol (DTT), 20 mM imidazole, 1 mg/mL lysozyme, 0.3 U/mL benzonase nuclease (Novagen), and Roche Complete EDTA-free protease inhibitor. The EcIspD wash buffer contained 20 mM Tris pH 7.5, 200 mM NaCl, 20 mM imidazole, and 1 mM $MgCl_2$. The elution buffer contained 140 mM NaCl, 14 mM Tris pH 7.5, 0.7 mM $MgCl_2$, and 314 mM imidazole.

Affinity-purified proteins were further purified over a HiLoad 16/60 Superdex 200 gel filtration column (GE Healthsciences) using an AKTAExplorer 100 FPLC (GE Healthsciences). FPLC buffer contained 250 mM NaCl, 25 mM Tris pH 7.5, and 1 mM $MgCl_2$. Fractions containing purified protein (>90% pure as evaluated by SDS-PAGE) were pooled and concentrated by centrifugation using Amicon Ultra-15 centrifugal filter units (EMD Millipore). Concentrated protein was supplemented with 1 mM DTT and 10% glycerol, flash frozen in liquid nitrogen, and stored at −80 °C. The protein concentration was measured using a BCA protein assay kit (Thermo Scientific).

***M. tuberculosis*.** The pETSUMO-IspD plasmid was transformed into *E. coli* BL21 cells. These BL21 cultures were grown at 37 °C until an OD_{600} of 0.6 was reached and then induced with 1 mM IPTG and grown 3 h at 37 °C. Cell pellets were lysed, and His-SUMO-IspD was purified by Ni^{2+} affinity chromatography. The fusion protein was eluted with 250 mM imidazole, the protein concentration was quantified, and the His-SUMO tag was cleaved off by incubation with purified His-Ulp1 protease. The His-Ulp-1, His-SUMO, and uncleaved His-SUMO-IspD protein were removed by subtractive Ni^{2+}-affinity chromatography. Purified MtIspD was then subjected to size exclusion chromatography as described above. The purity of each purified protein was assessed by SDS-PAGE (Figure S2).

IspD Assay Conditions. Phosphate released by IspD was quantified using the EnzChek phosphate assay kit (Invitrogen, Life Technologies) as previously described.[8] 2-Amino-6-mercapto-7- methylpurine riboside (MESG) and purine nucleoside phosphorylase (PNP) were diluted and stored according to the manufacturer's instructions. Final concentrations of reagents were as follows: 100 mM NaCl, 25 mM Tris pH 7.0, 7.5 mM $MgCl_2$, 1 mM DTT, 1 U/mL PNP, and 0.1 U/mL yeast inorganic pyrophosphatase (New England Biolabs). IC_{50} assays contained 50 μM CTP (Sigma), 500 μM MEP (Echelon Biosciences), 0.1% DMSO (vehicle for 1*R*,3*S*-MMV008138), and 0.2 mM MESG. Assays to determine kinetic parameters contained 0.0001% DMSO (vehicle for 1*R*,3*S*-MMV008138) and 0.4 mM MESG. In assays with variable CTP concentrations, 500 μM MEP was used; in assays with variable MEP concentrations, 500 μM CTP was used. Reactions were performed in 50 μL final volumes in 96-well clear, flat bottom plates and were initiated by the addition of purified MEP substrate to prewarmed enzyme and buffers. IspD enzyme concentrations were as follows: PfIspD, 50 nM; PvIspD, 50 nM; MtIspD, 100 nM; and EcIspD, 2 nM. Absorbance over time at 360 nm was measured on a BMG

DOI: 10.1021/id500047s
ACS Infect. Dis. 2015, 1, 157−167

POLARStar plate reader, preheated to 37 °C. Nonlinear regression analysis was performed using GraphPad Prism software, using data points from at least three independent experimental replicates. Slopes of changing absorbance values were converted to (μM MEP)(μM enzyme)$^{-1}$ s^{-1} using a phosphate standard curve.

Molecular Modeling. A homology model of PfIspD was constructed using the PHYRE online homology modeling program.[32] PfIspD primary sequence Q8I273 was obtained from UNIPROT (http://www.uniprot.org/, accessed 10/12/14). A number of protein alignments and homology models were constructed by PHYRE, and the model with 98.82% confidence was selected, which was based on an *E. coli* IspD structure (PDB accession code 1I52).[59] 1I52 is a 1.50-Å-resolution crystal structure of *E. coli* IspD, complexed with CDP-ME in the active site. The structure of the model was validated using the WHATIF web interface.[33]

1*R*,3*S*-MMV008138 was modeled in silico using the homology model described above in order to visualize the interactions between each analogue and the active site. Using GOLD, protons were added and docking was performed with default parameters, except that GoldScore was used and 50 docking poses were obtained for comparison and analysis.[34]

***P. falciparum* Culture.** Unless otherwise specified, *P. falciparum* parasites were cultured as previously described[40,60] in a 2% suspension of human erythrocytes in RPMI-1640 medium (Sigma-Aldrich) supplemented with 27 mM sodium bicarbonate, 11 mM glucose, 5 mM HEPES, 1 mM sodium pyruvate, 0.37 mM hypoxanthine, 0.01 mM thymidine, 10 μg mL^{-1} gentamicin, and 0.5% Albumax (Life Technologies). Cultures were maintained in 5% O_2/5% CO_2/90% N_2 at 37°. Parasite growth was monitored by the microscopy of Giemsa-stained parasites. Parasite strains used were as follows: 3D7 (Malaria Research and Reference Reagent Resource Center, ATCC, Manassas, VA); 3D7-IG (3D7-derived strain for genetic manipulation, kind gift from Daniel Goldberg, Washington University); AM1 (3D7-derived fosmidomycin-resistant clone, with *HAD1* loss-of-function allele[40]); and AM1 Hsp110: PfHAD1-GFP (strain AM1, complemented with a transposon-inserted HAD1-GFP expression construct[40]).

Genetic Validation of *PfISPD*. Functional genetic validation of *PfISPD* was performed as previously described for *PfDXR*.[12] In brief, pCAM-BSD-PfIspD^{KO} and pCAM-BSD-PfIspD^{control} vectors were derived from pCAM-BSD (gift from David Fidock, Columbia University), which includes a blasticidin-resistance cassette under transcriptional control by the *P. falciparum* D10 calmodulin 5′ UTR and the 3′ UTR of HRP2 from *P. berghei*. Both inserts were directly 5′ of the *P. berghei* DHFR-thymidylate synthase 3′ UTR.

To construct pCAM-BSD-PfIspD^{KO}, the coding sequence for a segment of PfIspD near the N-terminus (bp 17−645) was inserted directly into 5′ of the *P. berghei* DHFR-thymidylate synthase 3′ UTR. This insert was constructed by PCR using primers (A) 5′-GCTACTGCAGCGTTTATTCGTTGTGTTCTAC-3′ and (B) 5′-GCTACCCGGGCTTAGGACCGATCAATTCAG-3′ and restriction cloned using *Pst*I and *Sma*I sites. pCAM-BSD-PfIspD^{control} contained the coding sequence for the C-terminal end of PfIspD (bp1543−2205), generated using (C) 5′-GCTACTGCAGCATGATGGTGCTCGTCCT-3′ and (D) 5′-GCTACCCGGGCATCTTCTGGTGTAGTTAC-3′ as primers. This sequence was inserted at the same site, 5′ of the *P. berghei* DHFR-thymidylate synthase 3′ UTR. All constructs were verified by Sanger sequencing.

Transfections. pCAM-BSD-PfIspD^{KO} and pCAM-BSD-PfIspD^{control} plasmids were produced in *E. coli* (Invitrogen Top 10 cells). For transfection of the pCAM-BSD-PfIspD^{KO} and pCAM-BSD-PfIspD^{control} plasmids, 150 μg of plasmid was precipitated and resuspended in 400 μL of Cytomix (120 mM KCl, 0.15 mM $CaCl_2$, 2 mM EGTA, 5 mM $MgCl_2$, 10 mM K_2HPO_4, 25 mM HEPES, pH 7.6).

Four milliliters of 3D7-IG *P. falciparum* culture was synchronized by treatment with 5% sorbitol to obtain ring-stage parasites at >4% parasitemia. During transfection, cells were washed with Cytomix and resuspended in 400 μL of DNA/Cytomix solution. Cells were electroporated using a Biorad GenePulser II electroporator set to 950 μF capacitance and 0.31 kV. Transfected cells were washed with media and cultured as described. Culture media was replaced daily for 1 week. Beginning 48 h post-transfection, cultures were maintained under selection with 2 μg/mL blasticidin (Invitrogen, Life Technologies). To encourage integration at the *PfIspD* native locus, transfectant KO1 was cycled off blasticidin selection for a 2 week period, beginning approximately 1 month after transfection. Transfectant KO2 was cycled off blasticidin beginning approximately 2.5 months after transfection. After cycling off drug, treatment with blasticidin was resumed. Diagnostic PCRs were performed using genomic DNA from resultant transfectants using primer sets specific for episomal plasmids or genome integrants. Primer A and D sequences are given above: (X) 5′-TAAGAACATATTTATTAAACTGCAG-3′; (Y) 5′-GAAAAACGAACATTAAGCTGCCATA-3′.

Southern Blots. Southern blots were used to assay the integration of either the pCAM-BSD-PfIspD^{control} or the pCAM-BSD-PfIspD^{KO} plasmid. To assay the integration of pCAM-BSD-PfIspD^{KO}, genomic DNA was harvested from wild-type 3D7 *P. falciparum* and from cycled pCAM-BSD-PfIspD^{KO} transfectants KO1 and KO2 (see above). These genomic DNA samples, along with pCAM-BSD-PfIspD^{KO} plasmid, were digested with AccI and *Sma*I (New England Biolabs). The probe was prepared from PCR product generated using primers A and B (PfIspD bp 17−645) prior to southern blotting. To assay the integration of pCAM-BSD-PfIspD^{control}, genomic DNA was harvested from wild-type 3D7 *P. falciparum* and from the continuously cultured pCAM-BSD-PfIspD^{control} transfectant, C1 (see above). These genomic DNA samples, along with pCAM-BSD-PfIspD^{KO} plasmid, were digested with AccI and *Pst*I (New England Biolabs). The probe was prepared from PCR product generated using primers C and D (PF3D7_0106900 bp 1543−2205) prior to southern blotting.

Fosmidomycin and 1*R*,3*S*-MMV008138 Isobolograms. Asynchronous cultures of *P. falciparum* strain 3D7 were diluted to 0.5% parasitemia and cultured over a range of concentrations of 1*R*,3*S*-MMV008138 and/or fosmidomycin in 100 μL culture volumes. Stock solutions of fosmidomycin and 1*R*,3*S*-MMV008138 were prepared at concentrations such that the EC_{50} values for these compounds alone would fall around the midpoint of a 10-point 2-fold dilution series. As previously described,[38] drug response curves were then performed at fosmidomycin/1*R*,3*S*-MMV008138 ratios of 5:0, 4:1, 3:2, 2:3, 1:4, and 0:5. After 72 h, parasite growth was quantified using PicoGreen dye (Invitrogen) to measure the DNA content as previously described.[8] EC_{50} values were calculated, treating each fosmidomycin/1*R*,3*S*-MMV008138 combination as if it were a single unique drug, by nonlinear regression analysis using GraphPad Prism software. Following these calculations,

DOI: 10.1021/id500047s
ACS Infect. Dis. 2015, 1, 157−167

EC_{50} values were prorated between compounds according to fosmidomycin/1*R*,3*S*-MMV008138 ratios and plotted as an isobologram. Each data point represents the average of at least three independent experimental replicates.

Parasite Drug Sensitivity Assays. Asynchronous cultures of *P. falciparum* strains AM1 and AM1 Hsp110:PfHAD1-GFP were diluted to 1% parasitemia and cultured in the indicated concentrations of 1*R*,3*S*-MMV008138, 1*S*,3*R*-MMV008138, or fosmidomycin in 150 μL culture volumes. After 72 h, parasite growth was quantified using PicoGreen dye (Invitrogen) to measure the DNA content as previously described.[8] PicoGreen fluorescence was measured (485 nm excitation/528 nm emission) in a POLARStar Omega microplate reader (BMG Labtech). IC_{50} values were calculated by nonlinear regression analysis using GraphPad Prism software and reflect the mean and 95% confidence intervals of at least three independent replicates.

■ ASSOCIATED CONTENT

Ⓢ Supporting Information

The following file is available free of charge on the ACS Publications website at DOI: 10.1021/id500047s.

Sequence information for codon-optimized *Plasmodium* IspD, metabolite profiling of artemisinin and chloroquine-treated *P. falciparum*, SDS-PAGE analysis of purified IspD enzymes, determination of kinetic parameters for PfIspD mutants and PvIspD, and assessment of integration of single-crossover knockout and control vectors (PDF)

■ AUTHOR INFORMATION

Corresponding Author

*E-mail: odom_A@kids.wustl.edu. Tel: 314-747-2370. Fax: 314-286-2895.

Present Address

(L.S.I., K.M.M., L.X.L., and C.L.S.) Department of Molecular Microbiology, Washington University School of Medicine, Washington University School of Medicine, St. Louis, Missouri 63110, United States. (C.M.A., R.L.E., and A.R.O.) Department of Pediatrics, Washington University School of Medicine, St. Louis, Missouri 63110, United States. (M.C.M.) Department of Medicine, University of Chicago, Chicago, Illinois 60637, United States. (T.L.) College of Medicine, University of Toledo, Toledo, Ohio 43614, United States. (K.E.P., N.G.B., P.M.O.) Robert Robinson Laboratories, Department of Chemistry, University of Liverpool, Liverpool L69 7ZD, United Kingdom.

Author Contributions

Planned experiments: A.R.O., L.S.I., C.M.A., N.G.B., and C.L.S. Performed experiments: A.R.O., L.S.I., M.C.M., K.E.P., T.L., R.L.E., K.M.M., and L.X.L. Wrote article: L.S.I., C.M.A., A.R.O., C.L.S., N.G.B., K.E.P., and P.M.O.

Notes

The authors declare no competing financial interest.

■ ACKNOWLEDGMENTS

This work was supported by the Children's Discovery Institute of St. Louis Children's Hospital and Washington University (A.R.O., P.M.O., and N.G.B.). A.R.O. is additionally supported by NIH/NIAID R01 AI103280, a Basil O'Connor Starter Scholar Award (March of Dimes) and a Clinical Scientist Development Award (Doris Duke Charitable Foundation). L.S.I., R.L.E., and K.M.M. are supported by NIH Infectious Disease Training Grant no. AI007172, and K.M.M. is also supported by the Stephen I. Morse Graduate Fellowship. K.E.P. is supported by the Engineering and Physical Sciences Research Council. T.L. is supported by the Society for Pediatric Research and Alpha Omega Alpha Medical Honor Society. L.X.L. is supported by NIH MSTP training grant no. GM007200-38. C.L.S. is supported by a Beckman Young Investigator Award from the Arnold and Mabel Beckman Foundation. We are grateful to Dana M. Hodge for technical assistance and to Ann Guggisberg and Andrew Jezewski for helpful discussions. The pCAM-BSD vector was a gift from David Fidock (Columbia University). The 3D7-IG *P. falciparum* strain was provided by Daniel Goldberg (Washington University).

■ ABBREVIATIONS

DOXP, deoxyxylulose 5-phosphate; MEP, methylerythritol phosphate; CTP, cytidine triphosphate; CDP-ME, cytidine diphosphate-methylerythritol; IPP, isopentenyl pyrophosphate; DMAPP, dimethylallyl pyrophosphate; MEcPP, methylerythritol cyclic diphosphate

■ REFERENCES

(1) WHO. (2014) World Malaria Report 2014, World Health Organization.

(2) Muller, O., Sie, A., Meissner, P., Schirmer, R. H., Kouyate, B. Artemisinin resistance on the Thai-Cambodian border. *Lancet* 2009, *374*, 10.1016/S0140-6736(09)61857-2.

(3) Dondorp, A. M., Nosten, F., Yi, P., Das, D., Phyo, A. P., Tarning, J., Lwin, K. M., Ariey, F., Hanpithakpong, W., Lee, S. J., Ringwald, P., Silamut, K., Imwong, M., Chotivanich, K., Lim, P., Herdman, T., An, S. S., Yeung, S., Singhasivanon, P., Day, N. P., Lindegardh, N., Socheat, D., and White, N. J. (2009) Artemisinin resistance in *Plasmodium falciparum* malaria. *N. Engl. J. Med. 361*, 455−467.

(4) Ashley, E. A., Dhorda, M., Fairhurst, R. M., Amaratunga, C., Lim, P., Suon, S., Sreng, S., Anderson, J. M., Mao, S., and Sam, B. (2014) Spread of artemisinin resistance in *Plasmodium falciparum* malaria. *N. Engl. J. Med. 371*, 411−423.

(5) Programme W. H. O. G. M. Update on artemisinin resistance. January 2014, World Health Organization.

(6) Gershenzon, J., and Dudareva, N. (2007) The function of terpene natural products in the natural world. *Nat. Chem. Biol. 3*, 408−414.

(7) Odom, A. R. (2011) Five Questions about Non-Mevalonate Isoprenoid Biosynthesis, *PLoS Pathogens 7*, 10.1371/journal.-ppat.1002323.

(8) Zhang, B., Watts, K. M., Hodge, D., Kemp, L. M., Hunstad, D. A., Hicks, L. M., and Odom, A. R. (2011) A second target of the antimalarial and antibacterial agent fosmidomycin revealed by cellular metabolic profiling. *Biochemistry 50*, 3570−3577.

(9) Cassera, M. B., Gozzo, F. C., D'Alexandri, F. L., Merino, E. F., del Portillo, H. A., Peres, V. J., Almeida, I. C., Eberlin, M. N., Wunderlich, G., Wiesner, J., Jomaa, H., Kimura, E. A., and Katzin, A. M. (2004) The methylerythritol phosphate pathway is functionally active in all intraerythrocytic stages of *Plasmodium falciparum*. *J. Biol. Chem. 279*, 51749−51759.

(10) Cassera, M. B., Merino, E. F., Peres, V. J., Kimura, E. A., Wunderlich, G., and Katzin, A. M. (2007) Effect of fosmidomycin on metabolic and transcript profiles of the methylerythritol phosphate pathway in *Plasmodium falciparum*. *Mem. Inst. Oswaldo Cruz 102*, 377−383.

(11) Wiley, J. D., Merino, E. F., Krai, P. M., McLean, K. J., Tripathi, A. K., Vega-Rodríguez, J., Jacobs-Lorena, M., Klemba, M., and Cassera, M. B. (2014) Isoprenoid Precursor Biosynthesis is the Essential Metabolic Role of the Apicoplast during Gametocytogenesis in Plasmodium falciparum. *Eukaryotic Cell 14*, 128−139.

DOI: 10.1021/id500047s
ACS Infect. Dis. 2015, 1, 157−167

(12) Odom, A. R., and Van Voorhis, W. C. (2010) Functional genetic analysis of the *Plasmodium falciparum* deoxyxylulose 5-phosphate reductoisomerase gene. *Mol. Biochem. Parasitol. 170*, 108−111.
(13) Koppisch, A. T., Fox, D. T., Blagg, B. S., and Poulter, C. D. (2002) *E. coli* MEP synthase: steady-state kinetic analysis and substrate binding. *Biochemistry 41*, 236−243.
(14) Wells, T. N. (2012) New Medicines to Combat Malaria: An Overview of the Global Pipeline of Therapeutics. In *Treatment and Prevention of Malaria: Antimalarial Drug Chemistry, Action, and Use*; (Paquette, S., Krishna, S., Eds.; Springer: Basel; pp 227−247.
(15) Fujisawa Pharmaceutical Company, Ltd., *Hydroxyaminohydrocarbonphosphonic Acids*. U.S. Patent US4206156, 1978.
(16) Kuemmerle, H. P., Murakawa, T., Soneoka, K., and Konishi, T. (1985) Fosmidomycin: a new phosphonic acid antibiotic. Part I: Phase I tolerance studies. *Int. J. Clin. Pharmacol. Ther. Toxicol. 23*, 515−520.
(17) Wiesner, J., Borrmann, S., and Jomaa, H. (2003) Fosmidomycin for the treatment of malaria. *Parasitol. Res. 90*, S71−S76.
(18) Borrmann, S., Adegnika, A. A., Matsiegui, P. B., Issifou, S., Schindler, A., Mawili-Mboumba, D. P., Baranek, T., Wiesner, J., Jomaa, H., and Kremsner, P. G. (2004) Fosmidomycin-clindamycin for *Plasmodium falciparum* Infections in African children. *J. Infect. Dis. 189*, 901−908.
(19) Borrmann, S., Lundgren, I., Oyakhirome, S., Impouma, B., Matsiegui, P. B., Adegnika, A. A., Issifou, S., Kun, J. F., Hutchinson, D., Wiesner, J., Jomaa, H., and Kremsner, P. G. (2006) Fosmidomycin plus clindamycin for treatment of pediatric patients aged 1 to 14 years with *Plasmodium falciparum* malaria. *Antimicrob. Agents Chemother. 50*, 2713−2718.
(20) Murakawa, T., Sakamoto, H., Fukada, S., Konishi, T., and Nishida, M. (1982) Pharmacokinetics of fosmidomycin, a new phosphonic acid antibiotic. *Antimicrob. Agents Chemother. 21*, 224−230.
(21) Kuemmerle, H., Murakawa, T., Sakamoto, H., Sato, N., Konishi, T., and De Santis, F. (1985) Fosmidomycin, a new phosphonic acid antibiotic. Part II: 1. Human pharmacokinetics. 2. Preliminary early phase IIa clinical studies. *Int. J. Clin. Pharmacol., Ther., Toxicol. 23*, 521−528.
(22) Na-Bangchang, K., Ruengweerayut, R., Karbwang, J., Chauemung, A., and Hutchinson, D. (2007) Pharmacokinetics and pharmacodynamics of fosmidomycin monotherapy and combination therapy with clindamycin in the treatment of multidrug resistant falciparum malaria. *Malaria J. 6*, 70.
(23) Ruangweerayut, R., Looareesuwan, S., Hutchinson, D., Chauemung, A., Banmairuroi, V., and Na-Bangchang, K. (2008) Assessment of the pharmacokinetics and dynamics of two combination regimens of fosmidomycin-clindamycin in patients with acute uncomplicated falciparum malaria. *Malar J. 7*, 225.
(24) Gamo, F.-J., Sanz, L. M., Vidal, J., de Cozar, C., Alvarez, E., Lavandera, J.-L., Vanderwall, D. E., Green, D. V. S., Kumar, V., Hasan, S., Brown, J. R., Peishoff, C. E., Cardon, L. R., and Garcia-Bustos, J. F. (2010) Thousands of chemical starting points for antimalarial lead identification. *Nature 465*, 305−310.
(25) Spangenberg, T., Burrows, J. N., Kowalczyk, P., McDonald, S., Wells, T. N., and Willis, P. (2013) The open access malaria box: a drug discovery catalyst for neglected diseases. *PLoS One 8*, e62906.
(26) Bowman, J. D., Merino, E. F., Brooks, C. F., Striepen, B., Carlier, P. R., and Cassera, M. B. (2014) Antiapicoplast and Gametocytocidal Screening To Identify the Mechanisms of Action of Compounds within the Malaria Box. *Antimicrob. Agents Chemother. 58*, 811−819.
(27) Wu, W., Herrera, Z., Ebert, D., Baska, K., Cho, S. H., DeRisi, J. L., and Yeh, E. (2014) A chemical rescue screen identifies a *Plasmodium falciparum* apicoplast inhibitor targeting MEP isoprenoid precursor biosynthesis. *Antimicrob. Agents Chemother. 59*, 356−364.
(28) Bernal, C., Palacin, C., Boronat, A., and Imperial, S. (2005) A colorimetric assay for the determination of 4-diphosphocytidyl-2-C-methyl-D-erythritol 4-phosphate synthase activity. *Anal. Biochem. 337*, 55−61.
(29) Tsang, A., Seidle, H., Jawaid, S., Zhou, W., Smith, C., Couch, R. D. (2011) Francisella tularensis 2-C-methyl-D-erythritol 4-phosphate cytidylyltransferase: kinetic characterization and phosphoregulation, *PLoS One 6*, 10.1371/journal.pone.0020884.
(30) Shi, W., Feng, J., Zhang, M., Lai, X., Xu, S., Zhang, X., and Wang, H. (2007) Biosynthesis of isoprenoids: characterization of a functionally active recombinant 2-C-methyl-D-erythritol 4-phosphate cytidyltransferase (IspD) from *Mycobacterium tuberculosis* H37Rv. *J. Biochem. Mol. Biol. 40*, 911−920.
(31) Hale, I., O'Neill, P., Berry, M., Odom, N. G., and Sharma, R. (2012) The MEP pathway and the development of inhibitors as potential anti-infective agents. *Med. Chem. Commun. 3*, 418−433.
(32) Kelley, L. A., and Sternberg, M. J. (2009) Protein structure prediction on the Web: a case study using the Phyre server. *Nat. Protoc. 4*, 363−371.
(33) Vriend, G. (1990) WHAT IF: a molecular modeling and drug design program. *J. Mol. Graphics 8*, 52−56.
(34) Verdonk, M. L., Cole, J. C., Hartshorn, M. J., Murray, C. W., and Taylor, R. D. (2003) Improved protein−ligand docking using GOLD. *Proteins: Struct., Funct., Bioinf. 52*, 609−623.
(35) Richard, S. B., Bowman, M. E., Kwiatkowski, W., Kang, I., Chow, C., Lillo, A. M., Cane, D. E., and Noel, J. P. (2001) Structure of 4-diphosphocytidyl-2-C-methylerythritol synthetase involved in mevalonate-independent isoprenoid biosynthesis. *Nat. Struct. Mol. Biol. 8*, 641−648.
(36) Yu, M., Kumar, T. R., Nkrumah, L. J., Coppi, A., Retzlaff, S., Li, C. D., Kelly, B. J., Moura, P. A., Lakshmanan, V., Freundlich, J. S., Valderramos, J. C., Vilcheze, C., Siedner, M., Tsai, J. H., Falkard, B., Sidhu, A. B., Purcell, L. A., Gratraud, P., Kremer, L., Waters, A. P., Schiehser, G., Jacobus, D. P., Janse, C. J., Ager, A., Jacobs, W. R., Sacchettini, J. C., Heussler, V., Sinnis, P., and Fidock, D. A. (2008) The fatty acid biosynthesis enzyme FabI plays a key role in the development of liver-stage malarial parasites. *Cell Host Microbe 4*, 567−578.
(37) Vaughan, A. M., O'Neill, M. T., Tarun, A. S., Camargo, N., Phuong, T. M., Aly, A. S., Cowman, A. F., and Kappe, S. H. (2009) Type II fatty acid synthesis is essential only for malaria parasite late liver stage development. *Cell. Microbiol. 11*, 506−520.
(38) Fivelman, Q. L., Adagu, I. S., and Warhurst, D. C. (2004) Modified fixed-ratio isobologram method for studying in vitro interactions between atovaquone and proguanil or dihydroartemisinin against drug-resistant strains of *Plasmodium falciparum*. *Antimicrob. Agents Chemother. 48*, 4097−4102.
(39) Wiesner, J., Henschker, D., Hutchinson, D. B., Beck, E., and Jomaa, H. (2002) In vitro and in vivo synergy of fosmidomycin, a novel antimalarial drug, with clindamycin. *Antimicrob. Agents Chemother. 46*, 2889−2894.
(40) Guggisberg, A. M., Park, J., Edwards, R. L., Kelly, M. L., Hodge, D. M., Tolia, N. H., and Odom, A. R. (2014) A sugar phosphatase regulates the methylerythritol phosphate (MEP) pathway in malaria parasites. *Nat. Commun. 5*, 4467.
(41) Guiguemde, W. A., Shelat, A. A., Garcia-Bustos, J. F., Diagana, T. T., Gamo, F.-J., and Guy, R. K. (2012) Global Phenotypic Screening for Antimalarials. *Chem. Biol. 19*, 116−129.
(42) Plouffe, D., Brinker, A., McNamara, C., Henson, K., Kato, N., Kuhen, K., Nagle, A., Adrián, F., Matzen, J. T., and Anderson, P. (2008) In silico activity profiling reveals the mechanism of action of antimalarials discovered in a high-throughput screen. *Proc. Natl. Acad. Sci. U.S.A. 105*, 9059−9064.
(43) Macdonald, S., Willis, P., Kowalczyk, P., Spanenberg, T., Burrows, J. N., Wells, T. N. Screening of the MMV malaria box compounds against *Plasmodium falciparum, Trypanosoma cruzi and brucei, Leishmania infantum* and measurement of cytotoxicity. *ChEMBL*; DOI: 10.6019/CHEMBL2028040.
(44) Caffrey, C., Suzuki, B. Malaria Box Schistosomiasis Screening Data. *ChEMBL*; DOI: 10.6019/CHEMBL2363022.
(45) Meister, S., Plouffe, D. M., Kuhen, K. L., Bonamy, G. M., Wu, T., Barnes, S. W., Bopp, S. E., Borboa, R., Bright, A. T., and Che, J. (2011) Imaging of *Plasmodium* liver stages to drive next-generation antimalarial drug discovery. *Science 334*, 1372−1377.

DOI: 10.1021/id500047s
ACS Infect. Dis. 2015, 1, 157−167

(46) Sun, W., Tanaka, T. Q., Magle, C. T., Huang, W., Southall, N., Huang, R., Dehdashti, S. J., McKew, J. C., Williamson, K. C., and Zheng, W. (2014) Chemical signatures and new drug targets for gametocytocidal drug development. *Sci. Rep. 4*, 3743.
(47) Lucantoni, L., Duffy, S., Adjalley, S. H., Fidock, D. A., and Avery, V. M. (2013) Identification of MMV malaria box inhibitors of *Plasmodium falciparum* early-stage gametocytes using a luciferase-based high-throughput assay. *Antimicrob. Agents Chemother. 57*, 6050−6062.
(48) Duffy, S., and Avery, V. M. (2013) Identification of inhibitors of *Plasmodium falciparum* gametocyte development. *Malaria J. 12*, 408.
(49) Sanders, N. G., Sullivan, D. J., Mlambo, G., Dimopoulos, G., and Tripathi, A. K. (2014) Gametocytocidal Screen Identifies Novel Chemical Classes with *Plasmodium falciparum* Transmission Blocking Activity. *PLoS One 9*, e105817.
(50) Nair, S. C., Brooks, C. F., Goodman, C. D., Strurm, A., McFadden, G. I., Sundriyal, S., Anglin, J. L., Song, Y., Moreno, S. N., and Striepen, B. (2011) Apicoplast isoprenoid precursor synthesis and the molecular basis of fosmidomycin resistance in *Toxoplasma gondii*. *J. Exp. Med. 208*, 1547−1559.
(51) Kunfermann, A., Witschel, M., Illarionov, B., Martin, R., Rottmann, M., Höffken, H. W., Seet, M., Eisenreich, W., Knölker, H. J., and Fischer, M. (2014) Pseudilins: Halogenated, Allosteric Inhibitors of the Non-Mevalonate Pathway Enzyme IspD. *Angew. Chem., Int. Ed. 53*, 2235−2239.
(52) Witschel, M. C., Hoffken, H. W., Seet, M., Parra, L., Mietzner, T., Thater, F., Niggeweg, R., Rohl, F., Illarionov, B., Rohdich, F., Kaiser, J., Fischer, M., Bacher, A., and Diederich, F. (2012) Inhibitors of the herbicidal target IspD: allosteric site binding. *Angew. Chem., Int. Ed. 50*, 7931−7935.
(53) Lesch, J. E. Chemotherapy by Design. *A Master of Science History*; Springer, 2012; pp 275−295.
(54) Périgaud, C., Gosselin, G., and Imbach, J. (1992) Nucleoside analogues as chemotherapeutic agents: a review. *Nucleosides Nucleotides 11*, 903−945.
(55) el Kouni, M. H. (2003) Potential chemotherapeutic targets in the purine metabolism of parasites. *Pharmacol. Ther. 99*, 283−309.
(56) O'Brien, Z., and Fallah Moghaddam, M. (2013) Small molecule kinase inhibitors approved by the FDA from 2000 to 2011: a systematic review of preclinical ADME data. *Exp. Opin. Drug Metab. Toxicol. 9*, 1597−1612.
(57) Huang, D., Zhou, T., Lafleur, K., Nevado, C., and Caflisch, A. (2010) Kinase selectivity potential for inhibitors targeting the ATP binding site: a network analysis. *Bioinformatics 26*, 198−204.
(58) Alexandrov, A., Vignali, M., LaCount, D. J., Quartley, E., de Vries, C., De Rosa, D., Babulski, J., Mitchell, S. F., Schoenfeld, L. W., and Fields, S. (2004) A facile method for high-throughput co-expression of protein pairs. *Mol. Cell. Proteomics 3*, 934−938.
(59) Baer, R. (2001) With the ends in sight: images from the BRCA1 tumor suppressor. *Nat. Struct. Biol. 8*, 822−824.
(60) Trager, W., and Jensen, J. B. (1976) Human malaria parasites in continuous culture. *Science 193*, 673−675.

DOI: 10.1021/id500047s
ACS Infect. Dis. 2015, 1, 157−167